An Independent Analysis of Evidence for $\nu_\mu \leftrightarrow \nu_\tau$ Oscillations in the Super-Kamiokande Atmospheric Neutrino Data

Natalia Toro

Fairview High School
Boulder, Colorado

Intel Science Talent Search
November 16, 1998

Summary

This study analyzes data from the Super-Kamiokande detector and finds evidence for flavor oscillations, in which neutrinos, the least understood of all known fundamental physical particles, change from one type into another over time. Such oscillations would prove that neutrinos have non-zero mass, a result with profound implications for the standard model of quantum mechanics.

1 Introduction

Neutrinos are elementary particles that were hypothesized to exist in 1930 by Wolfgang Pauli in order to account for the missing energy and momentum that seemed to be lost in the beta decay of neutrons into protons and electrons. Neutrinos interact very little with matter—so little that, although billions of neutrinos pass through a human body every second, only one or two actually interact with the matter in the body over a whole lifetime. Because neutrinos interact so little, their existence, as evidenced by rare collisions with nucleons, was not proven until 20 years after Pauli proposed it [1]. To this day, neutrinos are the most elusive of the known fundamental particles. In 1968, results of an experiment performed to detect neutrinos emitted by solar fusion reactions indicated an observed neutrino flux that was less than half of what theory had predicted [2]. The first explanation proposed for this solar neutrino problem, and the most readily accepted at first, was that the predictions of the standard solar model were incorrect. But soon another theory was proposed to explain the neutrino deficit: *neutrino oscillations*, also known as flavor mixing [3].

Flavor mixing is a uniquely quantum phenomenon in which one type of neutrino actually turns into another type. According to the quantum-mechanical Standard Model, there are three different types, or flavors, of neutrinos: electron neutrinos (ν_e), muon neutrinos (ν_μ), and tau neutrinos (ν_μ). Each is associated with a charged lepton: the electron and its antiparticle the positron ($e^\pm$), the muon ($\mu^\pm$), and the tau lepton ($\tau^\pm$). In reactions that involve neutrinos, such as $\pi^- \to \mu^- + \bar{\nu}_\mu$ and $\mu^- \to e^- + \bar{\nu}_e + \nu_\mu$, the neutrinos interact with their corresponding leptons, and physicists use these reactions to define the flavor of a neutrino. The solar neutrino problem would be resolved if a neutrino could change from a flavor that a detector could see to a flavor that the detector couldn't see, in which case it would seemingly disappear. Such a result would have a fundamental impact on high-energy physics [2]. Flavor mixing is possible because of *superposition of states*, in which a particle has a mixture of observable properties. Just as Schrödinger's apocryphal cat is neither fully dead nor fully alive, but rather some of both, so a neutrino can be a mixture of two flavors that resolves into one or the other with a certain probability when forced, by a measurement, to assume a definite state.

Mathematically, a neutrino's state can be expanded in terms of definite eigenstates of flavor or of mass, which may or may not be the same. For simplicity, we ignore ν_e mixing, which is relatively insignificant on the length scale of the atmospheric neutrino problem, and consider only two neutrino flavors—ν_μ and ν_τ. In

this two-dimensional case, we can relate the flavor eigenstates and the mass eigenstates by the equations

$$|\nu_\mu\rangle = \cos\Theta|m_1\rangle + \sin\Theta|m_2\rangle \quad \text{and} \quad |\nu_\tau\rangle = \sin\Theta|m_1\rangle - \cos\Theta|m_2\rangle, \tag{1}$$

where $|m_1\rangle$ and $|m_2\rangle$ are the mass eigenstates, for some *mixing angle* Θ. Because the two mass eigenstates of the neutrino evolve somewhat differently with time, a neutrino will, with a certain probability, actually change flavor between its creation and its detection. As will be shown in Section 2, the probability that a neutrino created in a muon-associated reaction (e.g. the muon neutrino produced by the muon decay $\mu^- \rightarrow e^- + \bar{\nu}_e + \nu_\mu$) will change by this mechanism into a ν_τ after traveling a distance L is given by

$$P(\nu_\mu \rightarrow \nu_\tau) = \sin^2 2\Theta \sin^2\left(1.27\frac{\Delta m^2[\mathrm{eV}^2]L[\mathrm{km}]}{E[\mathrm{GeV}]}\right), \tag{2}$$

where Δm^2 is the difference in squares of the masses of the two neutrino mass eigenstates and E is the energy of the neutrino.

Not all neutrinos, however, are produced in solar fusion. *Atmospheric neutrinos* are produced when cosmic rays interact with atoms in the Earth's atmosphere, producing particles that decay into neutrinos and other fundamental particles. Unlike solar neutrinos, which are all $\bar{\nu}_e$'s, atmospheric neutrinos can be either ν_e or ν_μ or their anti-particles. Results from Super Kamiokande, a 50,000 ton water Čerenkov detector in Japan, indicate that these atmospheric neutrinos are oscillating from ν_μ to some other type of neutrino, probably ν_τ [6]. On June 5th, 1998, the Super Kamiokande researchers announced this result and their discovery of neutrino mass in a widely reported press release.

This project analyzes the neutrino interaction events detected in Super Kamiokande to provide an independent verification of the evidence for neutrino flavor mixing. This involves deriving the theoretical expectations for neutrino oscillations, first in a simple, idealized case, and then with fewer approximations. These theoretical calculations, together with empirical momentum distributions, are then used to calculate the effect of oscillations on the neutrino flux through the detector as a function of zenith angle, and the predictions are compared to the experimental results by means of a chi-squared regression. The results differ somewhat in detail from those obtained by Super-Kamiokande, but strongly imply that something is happening to the

neutrinos and that oscillations are one feasible explanation.

2 Mathematical Derivation of the Oscillation Formula

As an initial approximation, we assume that a neutrino travels at essentially the speed of light c, and has a definite momentum p.[1] To derive the neutrino oscillation formula in this case, we begin by assuming that a neutrino's state can be represented in terms of flavor eigenstates, in this case $|\nu_\mu\rangle$ and $|\nu_\tau\rangle$, or mass eigenstates $|m_1\rangle$ and $|m_2\rangle$. If the flavor and mass eigenstates are the same, then no oscillations occur, but if the eigenstates differ it is possible for a neutrino to evolve over time into a different flavor.

Because propagation over time depends on energy and, therefore, on mass, a relation between the flavor eigenstates and the mass eigenstates is needed in order to calculate the time evolution of a neutrino. In general, we can write flavor eigenstates as linear combinations of mass eigenstates:

$$|\nu_\mu\rangle = \alpha|m_1\rangle + \beta|m_2\rangle \quad \text{and} \quad |\nu_\tau\rangle = \gamma\Theta|m_1\rangle - \delta|m_2\rangle. \tag{3}$$

Using orthonormality of the kets within each basis, equation (3) becomes

$$|\nu_\mu\rangle = \cos\Theta e^{i\psi_1}|m_1\rangle + \sin\Theta e^{i\psi_2}|m_2\rangle \quad \text{and} \quad |\nu_\tau\rangle = \sin\Theta e^{i\psi_2}|m_1\rangle - \cos\Theta e^{i\psi_1}|m_2\rangle, \tag{4}$$

where the mixing angle Θ determines the amount of mixing between flavor and mass eigenstates, and hence the extent to which neutrinos will oscillate between flavors. Absorbing the phase angles ψ_1 and ψ_2 into the basis states, equation (4) becomes

$$|\nu_\mu\rangle = \cos\Theta|m_1\rangle + \sin\Theta|m_2\rangle \quad \text{and} \quad |\nu_\tau\rangle = \sin\Theta|m_1\rangle - \cos\Theta|m_2\rangle. \tag{5}$$

Now consider a neutrino created at time $t = 0$ in state $|\nu_\mu\rangle$. If we denote the state of a neutrino at time t after its creation by $|\nu(t)\rangle$, we can write $|\nu(t)\rangle$ as a linear combination of $|m_1\rangle$ and $|m_2\rangle$. Applying the

[1] These approximations will be removed in Appendix 8, where we show that they do not introduce any significant error.

time-dependent Schrödinger equation, we can describe the evolution of the neutrino over time by writing

$$\begin{aligned} \langle m_1|\nu(t)\rangle &= \langle m_1|\nu_\mu\, e^{-i(E_1 t-\mathbf{p}\cdot\mathbf{x})/\hbar}\rangle \\ &= \langle m_1|\nu_\mu\rangle\, e^{-i(E_1 t-\mathbf{p}\cdot\mathbf{x})/\hbar} \\ &= \cos\Theta\, e^{-i(E_1 t-\mathbf{p}\cdot\mathbf{x})/\hbar} \qquad (6) \\ \text{and}\quad \langle m_2|\nu(t)\rangle &= \langle m_2|\nu_\mu\, e^{-i(E_2 t-\mathbf{p}\cdot\mathbf{x})/\hbar}\rangle \\ &= \langle m_2|\nu_\mu\rangle\, e^{-i(E_2 t-\mathbf{p}\cdot\mathbf{x})/\hbar} \\ &= \sin\Theta\, e^{-i(E_2 t-\mathbf{p}\cdot\mathbf{x})/\hbar}, \qquad (7) \end{aligned}$$

where E_1 and E_2 are the energies of mass eigenstates $|m_1\rangle$ and $|m_2\rangle$. Then the amplitude for a $\nu_\mu \to \nu_\tau$ oscillation is given by:

$$\begin{aligned} \langle \nu_\tau|\nu(t)\rangle &= \langle \nu_\mu|m_1\rangle\langle m_1|\nu(t)\rangle + \langle \nu_\mu|m_2\rangle\langle m_2|\nu(t)\rangle \\ &= \sin\Theta\cos\Theta e^{-i(E_1 t-\mathbf{p}\cdot\mathbf{x})/\hbar} - \cos\Theta\sin\Theta e^{-i(E_2 t-\mathbf{p}\cdot\mathbf{x})/\hbar} \\ &= e^{i[\mathbf{p}\cdot\mathbf{x}-(E_1+E_2)t/2]/\hbar}\sin 2\Theta \quad i\sin\left(\frac{E_2-E_1}{2\hbar}t\right). \qquad (8) \end{aligned}$$

Thus, the probability of a $\nu_\mu \to \nu_\tau$ oscillation is:

$$P\left(\nu_\mu \to \nu_\tau\right) = |\langle \nu_\tau|\nu(t)\rangle|^2 = \sin^2 2\Theta \quad \sin^2\frac{E_2-E_1}{2\hbar}t. \qquad (9)$$

Using the relativistic equation

$$E = \sqrt{p^2+m^2} \approx p + \frac{m^2}{2p} \quad (\text{for } mc \ll p), \qquad (10)$$

we have

$$E_2 - E_1 \approx \frac{\Delta m^2}{2pc} \quad (\text{where } \Delta m^2 = m_2^2 - m_1^2), \qquad (11)$$

and

$$P(\nu_\mu \to \nu_\tau) = \sin^2 2\Theta \quad \sin^2 \frac{\Delta m^2 t}{4p\hbar c}. \tag{12}$$

Approximating the neutrino to be traveling at the speed of light c, we can write $t = L/c$, where L is the distance traveled by the neutrino from its creation to its detection. Then

$$\begin{aligned} P(\nu_\mu \to \nu_\tau) &= \sin^2 2\Theta \quad \sin^2 \frac{1}{4\hbar c}\frac{\Delta m^2 L}{E} \\ &= \sin^2 2\Theta \sin^2 \left(1.27 \frac{\Delta m^2[\mathrm{eV}^2] L[\mathrm{km}]}{E[\mathrm{GeV}]}\right). \end{aligned} \tag{13}$$

This result was derived independently as part of this study but is also found in the literature (eg. [5]).

3 The Super-Kamiokande Experiment

When a cosmic ray collides with a nucleon (proton or neutron) in the atmosphere, roughly 15 km above the surface, several pions are emitted. Neutrinos are formed during the decay of these pions, given by [4]:

$$\begin{array}{rlll} \pi^\pm[\sim 140\ \mathrm{MeV}] \to & \mu^\pm & [\sim 110\ \mathrm{MeV}] \ + \ \nu_\mu(\bar{\nu}_\mu)[\sim 30\ \mathrm{MeV}] & \\ & \downarrow & & \\ & \mu^\pm & \to \ e^\pm + \nu_e(\bar{\nu}_e)[\sim 37\ \mathrm{MeV}] + \bar{\nu}_\mu(\nu_\mu)[\sim 37\ \mathrm{MeV}] & \end{array} \tag{14}$$

Thus, unlike solar neutrinos, which are only $\bar{\nu}_e$, atmospheric neutrinos can be ν_e, ν_μ, or their corresponding anti-particles, with a ν_μ/ν_e ratio of about 2. These atmospheric neutrinos are produced with relativistic velocity and scattered in all directions. Because neutrinos are acted on by the weak force alone, most of them will pass through the Earth unscattered, without interacting with any other particles. But if a method can be devised to observe the interaction of even a small fraction of the neutrino flux, these data can be used to estimate the total neutrino flux.

One such method, that used by Super-Kamiokande, is water Čerenkov detection. Super-Kamiokande is a large tank buried under a mountain to reduce background noise from cosmic rays, filled with 50,000 tons of water, and surrounded by photo-multiplier tubes. Most neutrinos pass undetected through Super Kamiokande,

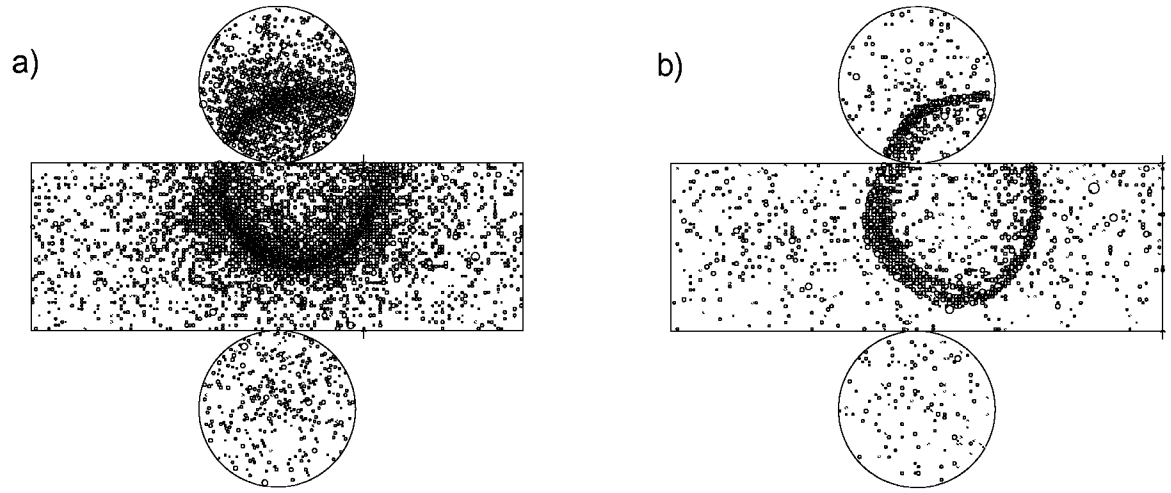

Figure 1: Images of Čerenkov cones produced by (a) electron-like and (b) muon-like interactions in Super-Kamiokande (modified from [9])

but some react in the water. The principal neutrino interaction that occurs in the detector is charged-current elastic scattering off a nucleon: $\nu + n \to l^- + p$ or $\bar{\nu} + p \to l^+ + n$, where the charged lepton l is an electron for an incident electron neutrino and a muon for an incident muon neutrino. The resulting relativistic leptons travel faster than the speed of light in water, and produce Čerenkov radiation—an electromagnetic shock wave analogous to the sonic boom that is observed whenever a body moves faster than the speed of sound. This radiation forms an expanding cone of light that leaves a ringed impression on the photo-multiplier tubes lining the edges of the detector.

By the nature of the weak interaction, the scattered lepton absorbs most of the energy of the neutrino, so the lepton four-momentum is a reasonable estimate of the four-momentum of the incoming neutrino that created it. There is, however, one additional consideration: whereas massive muons can pass through the water in the tank without losing all their energy, much lighter electrons often scatter many times before reaching the photo-multipliers. Thus the muon rings are clear and sharp, while the electron rings are much less clearly defined (see Figure 1). This difference allows physicists to determine the flavor of the lepton produced by the neutrino interaction, and hence the flavor of the incoming neutrino [7].

4 Data Analysis Procedure

4.1 Experimental Data

Two sets of data from Super-Kamiokande were used. The first is in the form of counts of neutrino interactions for four data sets (Sub-GeV e-like, Sub-GeV μ-like, Multi-GeV e-like, and Multi-GeV μ-like events) divided into five bins over $-1 \leq \cos\theta_z \leq 1$ [8]. The second set of data, histograms showing the momentum distribution of detected neutrinos in each of the four data sets [5], was used in calculating the expectation values for the interaction counts.

4.2 Calculation of Expected Neutrino Counts

Functions of the form

$$f(p) = C \cdot p^{\alpha}(p - p_0)^{\beta}, \tag{15}$$

were fitted to the experimental momentum distributions of Sub-GeV ${\nu_e}'s$, Sub-GeV ${\nu_\mu}'s$, Multi-GeV ${\nu_e}'s$, and Multi-GeV ${\nu_\mu}'s$ where p_0 is the minimum neutrino momentum for the sample in question. As the amount of data was small (only four data points in the worst case, the multi-GeV μ-like sample) and three parameters had to be fit, the validity of these fits is questionable. In addition, the data represent the distribution of momentum at the detector, whereas the formula calls for the distribution of the neutrinos when they are created. For a more accurate fit, the condition was imposed requiring that the quantity $\alpha + \beta$ agree with theoretical predictions [4], effectively reducing the number of fit parameters to two. Furthermore, since all results obtained from $f(p)$ are normalized, the constant C drops out. Finally, repeating the calculations with values of α and β significantly offset from the best fit, but maintaining the same sum, had no detectable effect on the results. Thus it is reasonable to conclude that, although it is not necessarily very accurate, the momentum distribution is satisfactory.

The oscillation probability (eqn. 2) is integrated numerically over momentum, weighted by this momentum distribution (eqn. 15), and normalized. For momentum in MeV, the probability that a neutrino drawn at random from the observed momentum distribution $f(p)$ does not change flavor before reaching Super-

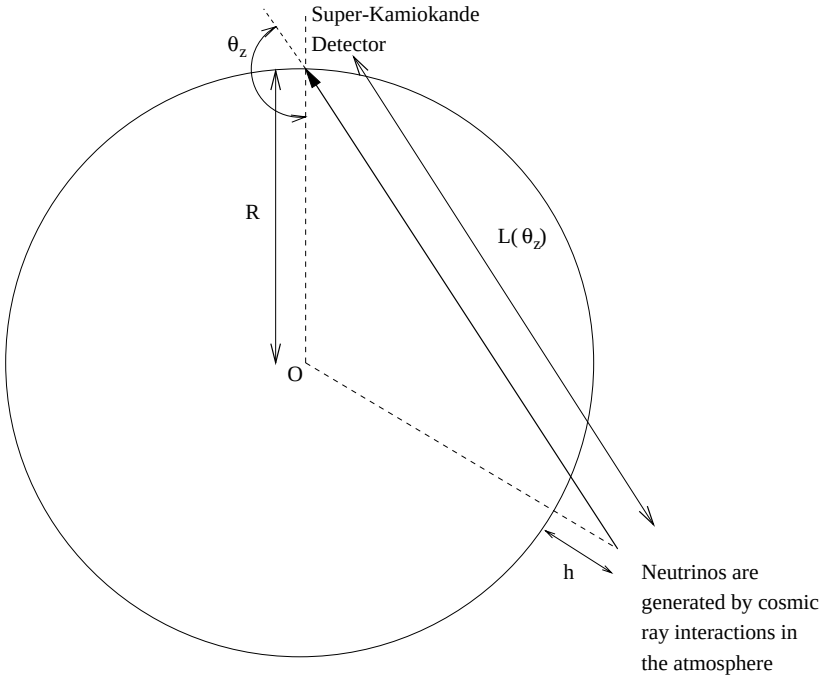

Figure 2: Geometric construction to find neutrino path length (not to scale)

Kamiokande is given by

$$P(\text{survival}) = \frac{\int dpf(p)\cos^2\left(1.27\Delta m^2 L(\theta_z)/pc\right)}{\int dpf(p)} \tag{16}$$

where $L(\theta_z) = \sqrt{R^2\cos^2\theta_z + 2Rh + h^2} - R\cos\theta_z$ is the neutrino path length, $h = 15$ km is the height at which neutrinos are created, the zenith angle θ_z is the angle between the vertical and the direction of the incoming neutrino, and R is the radius of the Earth. The depth of Super-Kamiokande (1 km) can be neglected.

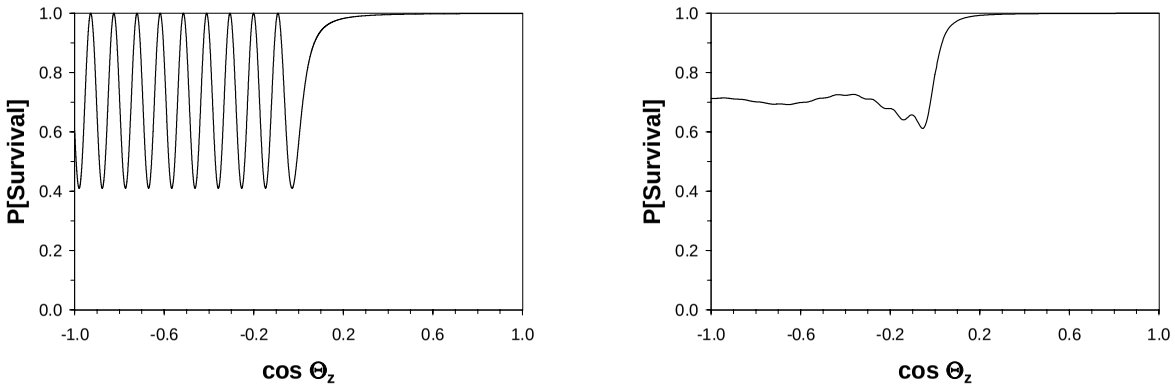

Figure 3: Theoretical survival probability of sub-GeV ν_μ as a function of zenith angle with $\Delta m^2 = 4.7 \cdot 10^{-4}\text{eV}^2, \sin^2(2\Theta) = 0.59$ (left) for p=300 MeV/c and (right) integrated over all p, weighted by f(p)

The effect of this integration is that, whereas the survival probability for a given momentum oscillates rapidly with zenith angle, as in Figure 3(left), the survival probability levels out when a range of momenta are considered. The resulting effect is a roughly even suppression of the survival probability to roughly $1 - \sin^2(2\Theta)/2$ for sufficiently large distances, as in Figure 3(right). Finally, these probabilities are multiplied by the expected neutrino flux distributions assuming no oscillations obtained from [8]. This distribution, dependent on the cosmic ray flux distribution, geomagnetic field, and interaction cross-sections for charged-current reactions, among other factors, is calculated using Monte Carlo simulations. The result is the expected neutrino count for given oscillation parameters.

4.3 Comparison of Theory and Experiment

The result of this process is a survival probability as a function of the zenith angle. But it is not yet in the proper form so that it can be compared to the experimental data. First, the experimental counts are given for five zenith-angle bins, whereas the theoretical survival probability is a continuous function of the zenith angle θ_z. Thus it is necessary to average the theoretical probability across each bin. Because this probability does not oscillate rapidly, ten sample points suffice to find this average. The theoretical survival probability is computed over a wide range of the oscillation parameters ($0 \leq \sin^2(2\Theta) \leq 1.0$ and $10^{-8}\,\text{eV} \leq \Delta m^2 \leq 1.0\text{eV}$) for 100 values of each parameter. A chi-squared goodness of fit test is then used to compare the theoretical calculations to the experimental data.

There are, however, two complications in this calculation, due to systematic uncertainties in the primary distribution of neutrinos created in the atmosphere. First, the correct overall normalization of the neutrino flux is not well known, with discrepancies among different models as great as 25%. It is assumed that the sub- and multi-GeV samples have the same normalization factor. This factor is accounted for by calculating the chi-squared statistic for many values of this normalization (from 0.5 to 1.5) and using that value for which the combined chi-squared statistic from both sub- and multi-GeV samples is least.

Not only is this overall normalization unknown, but there is also some uncertainty in the zenith-angle dependence of the normalization. This dependence is assumed to be linear with respect to $\cos\Theta_z$, with slope η. The value of η is taken to have a standard deviation of 2.7% for multi-GeV samples and 2.4% for sub-GeV samples [8]. The two data samples are allowed to have independent values of η, but they are not allowed to vary freely. Rather, the value of η is taken to have a standard deviation of 2.7% for multi-GeV samples and 2.4% for sub-GeV samples, and high values of η are penalized accordingly in calculating the chi-squared statistic. Incorporating the normalization and up-down asymmetry, the final result for the predicted count distribution is given by:

$$N\theta_z = N_{MC}(\theta_z) \times \frac{P[survival](\theta_z) \cdot (1 + \eta\cos(\theta_z))}{\alpha} \tag{17}$$

The total chi-squared statistic is obtained by summing the ten square deviations between theory and experiment (five from each momentum range) divided by their statistical variances and adding to this terms

for the up-down asymmetry and normalization coefficients. A chi-squared distribution with 8 degrees of freedom (10 data bins – 2 freely fitted parameters) is used to calculate, from this statistic, the probability that random error would result in discrepancies as large as those encountered. Repeating this process over a grid of parameters $(\sin^2(2\Theta), \Delta m^2)$, we have a measure for the goodness of fit as a function of these parameters. A similar process is applied to the sub-GeV and multi-GeV samples taken separately.

5 Results

Table 1 summarizes the results of the chi-squared analysis. The flux normalization α and the up-down asymmetry coefficient η that yield the best fit assuming no oscillations, together with the associated chi-squared statistic and probability, are shown for each of the four data samples, for both muon samples considered simultaneously, and for both electron samples considered simultaneously. The best-fit values of $\sin^2(2\Theta)$, Δm^2, α, and η for each of these samples, and the resulting chi-squared statistics and probabilities, are also shown. The number of degrees of freedom associated with each chi-squared probability is shown with the chi-squared statistic.

Summary of Chi-Squared Fits					
Sample	No Oscillation		Best Fit Parameters		
	α η	Fit Prob. (χ^2/dof)	$\sin^2(2\Theta)$ Δm^2[eV]^2	α η	Fit Prob. (χ^2 /dof)
Sub-GeV μ	138% 3.8%	0.000248 (19.2/3)	0.53 $3.05 \cdot 10^{-}5$	124% 0.3%	0.57 (2.02/3)
Multi-GeV μ	132% 3.8%	$5.9 \cdot 10^{-6}$ (27.3/3)	0.9 0.00242	96% -0.1%	0.998 (0.04/3)
All μ	136% [1] 3.9%, 3.6%	$8.17 \cdot 10^{-8}$ (48.5/8)	0.59 0.00047	114% [1]-0.6%,1.5%	0.108 (13.1/8)
Sub-GeV e	86% -1.6%	0.053 (7.67/3)	0.8 0.015	50% -0.8%	0.189 (4.78/3)
Multi-GeV e	112% 0.1%	0.44 (2.79/3)	0.02 0.99	82% -0.2%	0.44 (2.69/3)
All e	86% [1]-1.6%,-0.3%	0.2 (9.67/8)	0 ??[2]	86% [1]-1.6%,-0.3%	0.2 (9.67/8)

[1] First value is for Sub-GeV neutrinos, second is for Multi-GeV neutrinos

[2] Although the two states can have different mass, calculations for $\sin^2(2\Theta) = 0$ cannot help determine Δm^2 because the neutrinos do not oscillate

Table 1: Summary of Optimal Fits to Super-Kamiokande Data, With and Without Oscillation

In Figure 4, the experimental and predicted zenith-angle distributions (with and without oscillation) for $\nu_m u$ are compared assuming optimal parameters. The observed distribution, indicated by the points with error bars, and the Monte Carlo calculations, indicated by the shaded boxes, are the inputs to the problem. The dotted line represents the best possible fit to the data assuming no oscillations, the dashed line represents the best fit obtained using only the sample in question, and the solid line represents the fit obtained by combining both ν_μ samples.

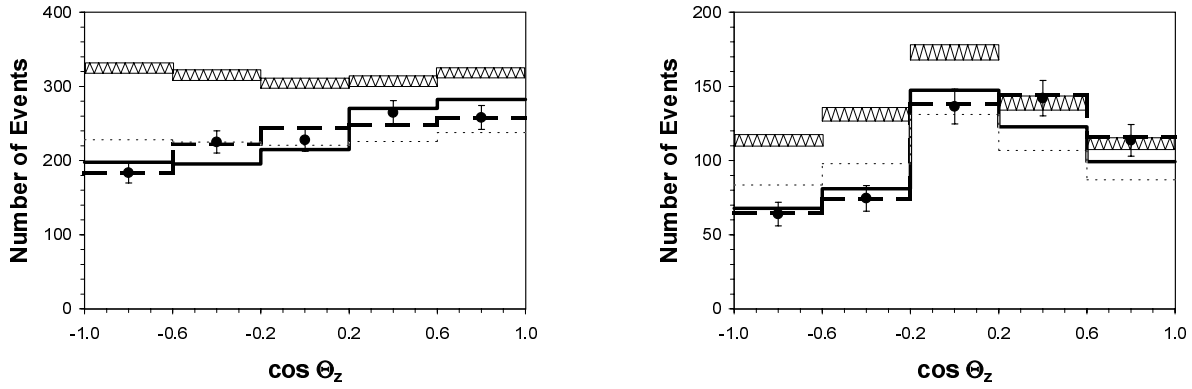

Figure 4: Zenith angle distributions of Super Kamiokande data (points with error bars), Monte Carlo predictions without oscillations (shaded boxes), best fit without oscillations(dotted lines), the optimal fit on the single sample with oscillations (dashed lines), and the optimal fit on both samples with oscillations (solid lines). Distributions are shown for (left) Sub-GeV and (right) Multi-GeV muon neutrino interaction

Figure 5 summarizes the region in $(\sin^2(2\Theta), \Delta m^2)$ space that yields chi-squared statistics within 90%, 95%, and 99% confidence bounds.

6 Discussion

6.1 Incompatibility of Data with No-Oscillation Model

The data from Table 1 and Figure 4 demonstrate convincingly that a no-oscillation solution is highly unlikely to produce the experimental results observed by Super-Kamiokande. The extreme values of α and η that result from assuming no oscillations tend to shift the expected results towards the lopsided distribution observed by

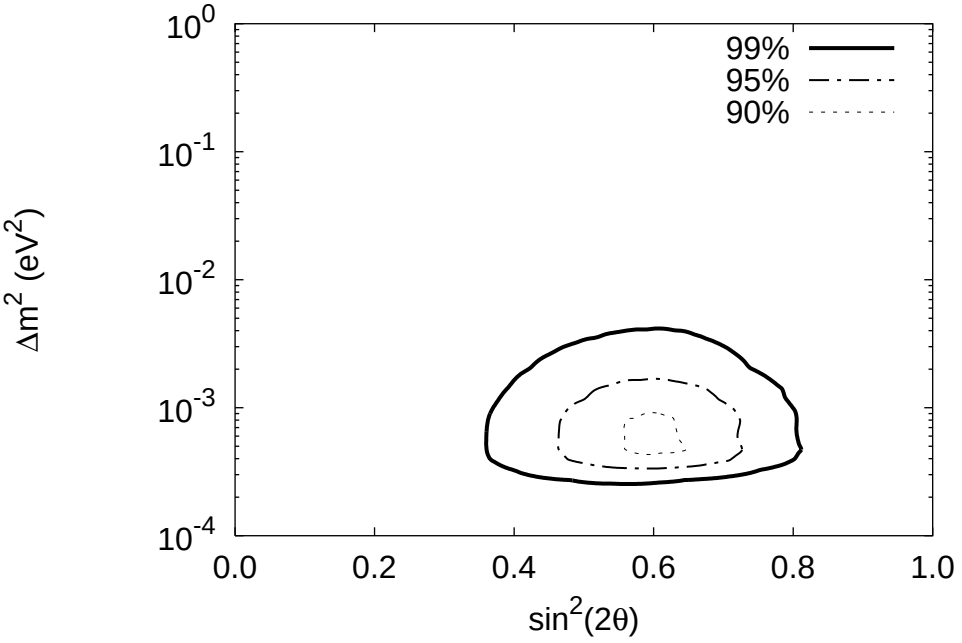

Figure 5: Acceptable range of $(\sin^2(2\Theta), \Delta m^2)$ at 90%, 95%, and 99% significance levels

Super Kamiokande, as in Figure 4. Even so, the probability of obtaining data as distant from the predicted values as the Super Kamiokande results is just under one in ten million. Such a low probability strongly suggests that the discrepancy between the Super Kamiokande data and the Monte Carlo predictions is due to some factor other than error in the normalization and up-down asymmetry of the atmospheric neutrino flux.

The data for electron neutrinos, however, is not indicative of significant oscillations. The no-oscillation hypothesis fits the data reasonably well. Assuming no oscillation, one would expect Super Kamiokande data to differ as much as they do (or more) from predictions with 20% probability. Furthermore, the best fit to the data occurs with no flavor mixing. Although the best fit to the multi-GeV data alone has significant mixing, these parameters fail for the sub-GeV sample, for which the resulting chi-squared statistic is roughly 470. Thus the sub-GeV data exclude this value of the parameters, while permitting low-mixing solutions which fare only slightly worse in the multi-GeV case.

This is not necessarily an indication that electron neutrinos do not mix at all with the other flavors. While this is one possibility, it is entirely possible that the electron neutrinos are mixing, possibly with a high value of $\sin^2(2\Theta)$, but that Δm^2 is too small to cause significant oscillations over the distances traveled by atmospheric

neutrinos, on the order of the Earth's diameter. The observed solar neutrino data would tend to favor the latter of these possibilities. Nevertheless, the data considered here provides no indication that factors other than normalization and up-down asymmetry are affecting the results significantly.

One might suggest that there is no quantum-mechanical mixing causing the observed discrepancy between experimental and predicted ν_μ distributions, but that the discrepancy can be explained by errors in the model of the cosmic ray interactions that produce atmospheric neutrinos. Although there is a systematic error of 25% in the atmospheric neutrino flux, this error is reasonably well accounted for by permitting variation in the parameters α and η. Furthermore, such an error would affect the muon and electron neutrino data in a nearly identical fashion. Thus error in the model of the production of the neutrinos is not sufficient to explain the observed effects, and there is strong evidence for another, more fundamental factor.

6.2 Possible Resolutions of the Disagreement

One solution to the large discrepancy between the predictions and experimental result observed for muon neutrinos is oscillation with another species of neutrinos, either ν_τ or ν_s, a hypothetical "sterile" neutrino flavor that does not interact with matter. Such oscillations would, as shown in Table 1, reasonably explain the distribution observed by Super Kamiokande. The two possible oscillation partners are indistinguishable, however, without a means of measuring ν_τ's, such as neutral-current interactions (used in [**?**] to disfavor $\nu_\mu \leftrightarrow \nu_\tau$ oscillations) or an altogether different detector, such as the heavy-water detector currently under construction in Sudbury, Canada.

Another possible explanation is neutrino decay, a somewhat more complex phenomenon. As in the simple oscillation case, mass and flavor eigenstates are allowed to mix. In addition, ν_2, the dominant component of ν_μ, is unstable and decays into ν_3. Such a situation, with rest-frame lifetime τ_0, can also account for the observations of Super Kamiokande [10]

6.3 Comparison of Parameters with those Determined by Super Kamiokande

The values obtained by this study for the oscillation parameters are $\sin^2(2\Theta) = 0.59, \Delta m^2 = 4.7 \cdot 10^{-4}\text{eV}^2$, whereas those obtained by Super Kamiokande are $\sin^2(2\Theta) = 1.0, \Delta m^2 = 2.2 \cdot 10^{-3}\text{eV}^2$. Why such a large

difference? Several differences between the analysis of this study and that of the Super Kamiokande collaboration can explain this discrepancy. These differences are in part due to the limitations on the data available for this study. Whereas the data used in the Super Kamiokande analysis was subdivided into five zenith-angle bins and fourteen momentum bins, the data used in this study was that presented in the published results of Super Kamiokande, which was grouped into the same five zenith angle bins but only two momentum bins (sub- and multi-GeV). Thus, through the coarser binning, a substantial amount of information was lost.

In addition to using less information, the model for this study was considerably simpler than that used in the Super Kamiokande analysis. Given the constraints on this study and the complexity of the calculations involved, Monte Carlo flux calculations were not performed. Instead, the model used in this study relied on the momentum and zenith-angle distributions obtained from the Super Kamiokande Monte Carlo simulation. As such, the momentum and zenith-angle distributions were considered to be independent, which is a physically inaccurate assumption. Furthermore, the height at which the neutrinos are produced is not constant at 15 km above the surface. In fact, not only is the height of production spread over a range of heights, but this range is dependent on the momentum of the neutrino. This issue is particularly significant for near-horizontal neutrinos, where this height-momentum dependence is most important, and even more so because this central region is very sensitive to Δm^2.

The first consideration, coarse binning of the data, would probably flatten the chi-squared distribution, but it would not, in general, result in radical changes in the best-fit parameters. The second, however, could lead to biases in the results. In support of this explanation for the discrepancy, we note that the results of this study for multi-GeV neutrinos were considerably closer to those of Super Kamiokande than the sub-GeV neutrino results. Because the particles involved in the creation of sub-GeV neutrinos have lower energies, effects such as the geomagnetic field, which would complicate the relationships between momentum and zenith-angle distributions, are much more significant than they are for multi-GeV neutrinos. Thus one would expect the sub-GeV results, for which the assumption of independence is less tenable, to differ more from the Super Kamiokande results than do the multi-GeV results. In spite of the discrepancy in the values for $\sin^2(2\Theta)$ and Δm^2 obtained by this study and by the Super Kamiokande analysis, both reach the same conclusion—that error in the atmospheric momentum flux alone cannot explain the Super Kamiokande atmospheric neutrino data, and

that the observed asymmetry and discrepancy with predictions is consstent with the oscillation hypothesis as well as other similar phenomena.

7 Conclusion

This study outlines theoretical calculations for two-state neutrino oscillation under the standard approximations and after removing some of these approximations (see Appendix 8). It provides evidence, through analysis of the Super Kamiokande neutrino oscillation data, for some neutrino mixing scenario and demonstrates that two-state ($\nu_\mu \leftrightarrow \nu_\tau$) oscillations are an acceptable solution to the atmospheric neutrino problem. It analyzes possible sources of the observed discrepancy between Super Kamiokande's results and those presented here, and concludes that the two analyses are not inconsistent.

8 Acknowledgments

I would like to thank my mentor, Professor Edmund Bertschinger of the Massachusetts Institute of Technology for his time and patience in directing me through this research. I would also like to thank Mrs. Joann P. DiGennaro and the Center for Excellence in Education for inviting me to the Research Science Institute (RSI) and allowing me the opportunity to do this research. I am also thankful to the RSI alumni who gave me advice, support, and editing assistance throughout the process of writing this paper, particularly to Rhiju Das, who offered many helpful suggestions as I expanded on my research after RSI. Finally, I am grateful to my parents, teachers, and friends who encouraged me to persevere during and after RSI.

References

[1] Reines, F., Cowan, C. L. Physical Review **113**, 273 (1959)

[2] Haxton, W. C.,"The Solar Neutrino Problem," Annu. Rev. Astron. Astrophys., 33:459-503 (1995)

[3] Bahcall, J. N. *Neutrino Astrophysics*, Cambridge: Cambridge University Press (1990).

[4] Honda, M., Kajita, T., Kasahara, K., Midorikawa, S. "Calculation of the Flux of Atmospheric Neutrinos" Phys. Rev. **D 248** (1995) 4985.

[5] Super-Kamiokande collaboration, M. Shiozawa, *Measurements of Atmospheric Neutrinos in the Super-Kamiokande Detector*, presented at Moriond E/W in France (March 1998)

[6] Fukuda, Y. et al, "Measurement of a small atmospheric ν_μ/ν_e ratio," Phys. Lett. B, in press (1998).

[7] Nakahata, M. et al, "Atmospheric neutrino Background and Pion Nucler Effect for KAMIOKA Nucleon Decay Experiment" J. Phys. Soc. of Japan 55:3786(1986)

[8] Kajita, T. for the Super-Kamiokande and Kamiokande collaborations, "Atmospheric neutrino results from Super-Kamiokande and Kamiokande—Evidence for ν_μ oscillations—" Proceedings of XVIII International Conference on Neutrino Physics and Astrophysics (Neutrino '98) in Takayama, Japan (June 1998)

[9] Itow, Y. representing Super-Kamiokande Collaboration, "Result in Neurino Oscillations from 400-Days Data of Super-Kamiokande" Talk given at topical conference at SLAC Summer Institute, Aug. 1997

[10] Barger, V., Learned, J. G., Pakvasa, S., and Weiler, T. J., "Neutrino Decay as an Explanation of Atmospheric Neutrino Observations" ??

[11] Gaisser, T. K., Stanev, T., "Pathlength Distributions of Atmospheric Neutrinos"

A Mathematical Derivation of the Oscillation Formula for Neutrinos with Gaussian Momentum Wavepackets

NOTE: I'm hoping to make some substantial additions and modifications to this appendix

This is the standard oscillation formula, but its derivation required several approximations, taking the speed of the neutrinos to equal c and assuming a definite momentum. Neither of these assumptions, however, is strictly true. Assuming they have mass, neutrinos travel at a speed that is somewhat less than the speed of light, and their momenta are not definite, but rather given distributed as a Gaussian wave-packet. The state of a neutrino is given by:

$$|\nu(t)\rangle = \int d^3p \sum_1^n \psi_i(\mathbf{p})|m_i, \mathbf{p}\rangle, \tag{18}$$

and the probability amplitude for a muon neutrino to remain a muon at $(\mathbf{x}, t)$ is:

$$\begin{aligned}
\langle \nu_\mu, \mathbf{x}|\nu(t)\rangle \quad &= \int d^3p \quad (2\pi\hbar)^{-3/4}\, e^{-(p-p_0)^2/4\sigma_p^2} \\
&\qquad \left(\cos^2\theta\; e^{-iE_1(t-t_0)/\hbar} + \sin^2\theta\; e^{-iE_2(t-t_0)/\hbar}\right) e^{ip\cdot x/\hbar} \\
&= (2\pi\hbar)^{-3/4} \quad \left[\cos^2\theta\; I(m_1) + \sin^2\theta\; I(m_2)\right],
\end{aligned} \tag{19}$$

where

$$I(m_i) = e^{i\left[\mathbf{p_0}\cdot\mathbf{x} - E_i(\mathbf{p_0})\right]/\hbar} \int d^3p e^{-p^2/4\sigma_p^2} e^{i\{\mathbf{p}\cdot\mathbf{x} - [E_i(p) - E_i(p_0)]/\hbar\}}. \tag{20}$$

To include possible effects of a finite-width wave packet, E(p) should be expanded to at least second order about the central momentum $\mathbf{p_0}$:

$$E(\mathbf{q}+\mathbf{p_0}) - E(\mathbf{p_0}) = \mathbf{q}\cdot\mathbf{p_0} + \frac{[q^2 - (\mathbf{q}\cdot\mathbf{v_0})^2]/2}{E(\mathbf{p_0})} + O(p^3),$$

where $\mathbf{q} = \mathbf{p} - \mathbf{p_0}$ is the displacement from the central momentum vector $\mathbf{p_0}$ and $\mathbf{v} = \mathbf{p_0}/E(\mathbf{p_0})$ is the group velocity of the wave packet. Rearranging terms, completing the square, and integrating, we have

$$
\begin{aligned}
I(m) \quad &= e^{i\left[\mathbf{p_0}\cdot\mathbf{x}-E_i(p_0)\right]/\hbar} \quad \int_{-\infty}^{\infty} dq_1 e^{-q_1^2/4\sigma_p^2+iq_1x_1/\hbar-itq_1^2/2E_0\hbar} \\
&\qquad \times \int_{-\infty}^{\infty} dq_2 e^{-q_2^2/4\sigma_p^2+iq_2x_2/\hbar-itq_2^2/2E_0\hbar} \\
&\qquad \times \int_{-\infty}^{\infty} dq_3 e^{-q_3^2/4\sigma_p^2+iq_3(x_3-vt)/\hbar-itq_3^2(1-v^2)/2E_0\hbar}
\end{aligned}
$$

$$
= e^{i\left[\mathbf{p_0}\cdot\mathbf{x}-E_i(p_0)\right]/\hbar+i\epsilon\sigma_p^2\left[\frac{x_1^2+x_2^2}{1+\epsilon^2}+\frac{(x_3-v_3t)^2(1-v^2)}{1+(1-v^2)\epsilon^2}\right]/\hbar^2} \; e^{-\sigma_p^2\left[\frac{x_1^2+x_2^2}{1+\epsilon^2}+\frac{(x_3-v_3t)^2}{1+(1-v^2)\epsilon^2}\right]/\hbar^2}, \tag{21}
$$

where $\epsilon = 2t\sigma_p^2c^2/(E_0\hbar)$.

For $\epsilon \ll 1$, equation (21) is not significantly different from equation (13). For atmospheric neutrinos, an upper bound for ϵ is on the order of 10^{-9}. This is small enough that it is reasonable to ignore the effect of the Gaussian momentum distribution on neutrino oscillations, and use equation (13) in the analysis. In other words, the wavepacket nature of momentum does not significantly affect state mixing and the neutrino behaves as if it was in a momentum eigenstate.